ELSEVIER

Powder Technology 92 (1997) 89–99

POWDER TECHNOLOGY

Particle collection efficiency of the rotational particle separator

J.J.H. Brouwers

Department of Mechanical Engineering, University of Twente, PO Box 217, 7500 AE Enschede, The Netherlands

Received 19 October 1995; revised 15 October 1996

Abstract

The rotational particle separator is a patented technique for separating solid and/or liquid particles of 0.1 μm and larger from gases. The core component is the rotating filter element which consists of a multitude of axially oriented channels which rotate as a whole around a common axis. Particles in the gas flowing in a laminar fashion through the channels are centrifuged towards the outer collecting walls of each individual channel while the purified gas leaves the channels at the exit. Solutions in closed form are presented for the probability that particles of given diameter are separated from the gas. Particle trajectories are governed by centrifugal forces and Stokes drag forces including Cunningham's correction. Solutions are given for channels of the following cross-sectional shapes: concentric rings, circles, triangles and sinusoids. Account has been taken of parabolic (Hagen–Poiseuille type) velocity distributions inside the channels and various distributions of the flow over the assembly of channels. The results compare favourably with measurements executed on six differently sized practical versions of the rotational particle separator.

Keywords: Separation; Rotational separators; Collection efficiency; Axial channels; Particle diameter measurement

1. Introduction

Recently, the rotational particle separator was introduced as a new technique for separating solid and/or liquid particles of 0.1 μm and larger from gases [1]. The technique can serve as an alternative to existing methods based on application of filter media, electrostatic precipitation, or wet scrubbing [2–4]. Practical designs of the rotational particle separator available on the market include equipment for purifying gases of industrial processes and portable air cleaners for domestic appliances.

The core component of the rotational particle separator is the rotating filter element (Fig. 1). It consists of a large number of axially oriented channels which rotate as a whole around a common axis. Solid and/or liquid particle material present in the gas flowing through the channels is centrifuged towards the outer collecting walls (Fig. 2). The purified gas leaves the channels while separated particle material adheres to the collecting walls as a result of the action of centrifugal forces, van der Waals forces and/or forces due to surface tension.

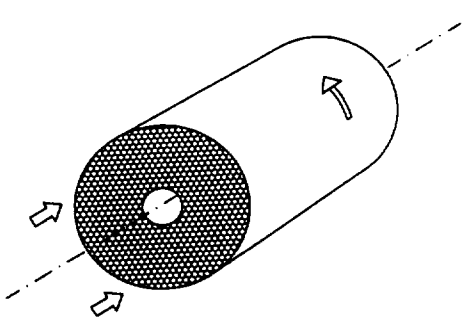

Fig. 1. Filter element of the rotational particle separator.

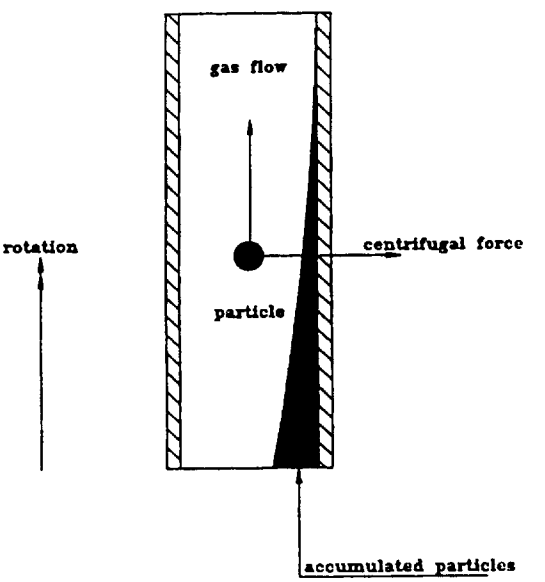

Fig. 2. Particle separation in a channel of the rotational particle separator.

PII S0032-5910(96)03251-2

In this paper an analysis is presented of the process of centrifugally induced particle separation of particles from the gas flowing through the channels of the rotational particle separator. Theoretical expressions are derived for the particle collection efficiency as a function of particle diameter, taking into account the channel shape, parabolic velocity profile inside the channel, distribution of the flow over the assembly of channels, and effects of molecular movement. Theoretical expressions are compared with results of measurements executed on a number of rotational particle separators under varying conditions.

2. Elementary separation

The channels of the rotational particle separator are designed such that laminar flow exists [1]. At entry or soon after, the gas will co-rotate with the filter element and flow in an axial direction parallel to the walls of the channels. As we are concerned with micrometre sized particles, forces associated with the inertia of the particles are small. Particles can be assumed to follow the streamlines of the gas with the exception of the radial direction where, as a result of the centrifugal force, particles move radially relative to the gas. The velocity at which particles move radially can be calculated on the basis of equilibrium between the centrifugal force and the drag force according to Stokes' law. Stokes' law describes the resistance due to the relative motion between a particle and the gas [5,6]. The equilibrium of forces can be expressed as

$$\frac{\pi}{6}\rho_p d_p^3 \Omega^2 r = 3\pi\eta d_p u_p \tag{1}$$

where ρ_p is the specific mass of the particle, d_p the particle diameter or equivalent diameter in the case of non-spherical particles, Ω the angular velocity, r the distance between the channel and the rotation axis, η the dynamic viscosity of the gas and u_p the radial velocity of the particle.

From Eq. (1) one obtains

$$u_p = \frac{\rho_p d_p^2 \Omega^2 r}{18\eta} \tag{2}$$

Whether a particle reaches the outer collecting wall of the channel depends on the residence time in the channel and the radial distance to be travelled by the particle. The smallest particle which is just able to reach the outer collecting wall with 100% probability is the particle which in the available time moves over a radial distance corresponding to the maximum height of the channel. Assuming uniform axial velocity over the channel cross-section, the radial velocity of this particle is

$$u_{p100\%} = w_{gas} d_c / L \tag{3}$$

where w_{gas} is the axial gas velocity in the channel, d_c the maximum channel height and L the channel length.

From Eqs. (2) and (3) an expression can be derived for the smallest particle which is collected with 100% probability in a channel located at radial position r, i.e.

$$d_{p100\%} = \left(\frac{18\eta w_{gas} d_c}{\rho_p \Omega^2 r L}\right)^{1/2} \tag{4}$$

From this formula it is noted that for constant values of d_c, w_{gas} and L, $d_{p100\%}$ increases with decreasing distance r from the rotation axis. This increase of $d_{p100\%}$ can be avoided by designing an axial gas velocity w_{gas} which increases linearly with distance r from the rotation axis. The reduction in centrifugal force with decreasing r is then compensated by an increase in residence time in the channel. The result is that the degree of particle separation will be the same for all channels. The desired distribution of the axial gas velocity can be accomplished by appropriate dimensioning of the inlet and outlet configuration upstream and downstream of the filter element.

In the case of an optimum distribution of the axial gas velocity, i.e. $w_{gas} \propto r$, an expression for $d_{p100\%}$ can be derived from Eq. (4) which is applicable to the entire filter element:

$$d_{p100\%} = \left(\frac{27\eta\phi d_c}{\rho_p \Omega^2 L \pi (1-\epsilon)(R_o^3 - R_i^3)}\right)^{1/2} \tag{5}$$

where ϕ is the gas flow through the filter element, ϵ the reduction of the effective cross-sectional area of the element due to the wall thickness of the channels, R_o the outer radius of the element and R_i the inner radius.

Consider the following example:

$\phi = 1\ m^3/s$	$L = 0.6\ m$	$R_i = 0.1\ m$
$d_c = 2\times10^{-3}\ m$	$\epsilon = 0.1$	$\rho_p = 2000\ kg/m^3$
$\Omega = 150\ rad/s$	$R_o = 0.3\ m$	$\eta = 1.8\times10^{-5}\ kg/m\ s$

In this case one calculates

$$d_{p100\%} = 7\times10^{-7}\ m$$

In other words, under the given conditions all particles with a diameter of 0.7 μm and larger are separated in the rotating filter element considered, Brownian motion being neglected. This result is obtained with a relatively small element: the residence time is less than 0.2 s. Furthermore, the circumferential speed of the element is limited to 45 m/s, resulting only in low friction and mechanical loading. According to the Hagen–Poiseuille formula for circular tubes [5,6], the pressure drop over the channels is assessed as 320 Pa.

3. Separation as a function of particle size for a single channel

It follows from the previous analysis that particles entering a separation channel will be collected with 100% probability when the diameter of these particles is larger than the value of $d_{p100\%}$ calculated for that channel according to Eq. (4). Also, particles smaller than $d_{p100\%}$ can reach the outer collecting wall provided that the distance of the particle from

the wall when entering the separation channel is sufficiently small. In general, the particle collection efficiency or collection rate, i.e. the percentage of particles of a certain diameter which will reach the wall, will decrease with the degree by which these particles are smaller than $d_{p100\%}$. In this section theoretical expressions will be derived for the particle collection efficiency as a function of particle diameter considering a single channel. Motivated by practical embodiments of the rotational particle separator, attention is focused on channels of the following shapes: concentric rings, circles, triangles and sinusoidal waves.

The situation where the axial velocity of the gas and particles is uniformly distributed over the channel cross-section is considered. The height of the channel is small in comparison with its distance from the rotation axis. Assume now that all particles with a certain diameter d_p are homogeneously distributed over the cross-sectional area at the entrance of any separation channel. Moving with the gas through the channel, all the particles will move with the same velocity in the radial direction. If a collecting wall were absent, at the exit of the separation channel two cross-sectional areas would be distinguished (Fig. 3): the cross-sectional area of the separation channel itself and the cross-sectional area formed by the particles of diameter d_p. As all particles considered have the same diameter d_p, they have all moved radially over the same distance t. The shape of the cross-sectional area formed by these particles is exactly the same as that of the cross-sectional area of the channel. The ratio of the number of particles which do not reach the wall to all particles initially present in the cross-sectional area at

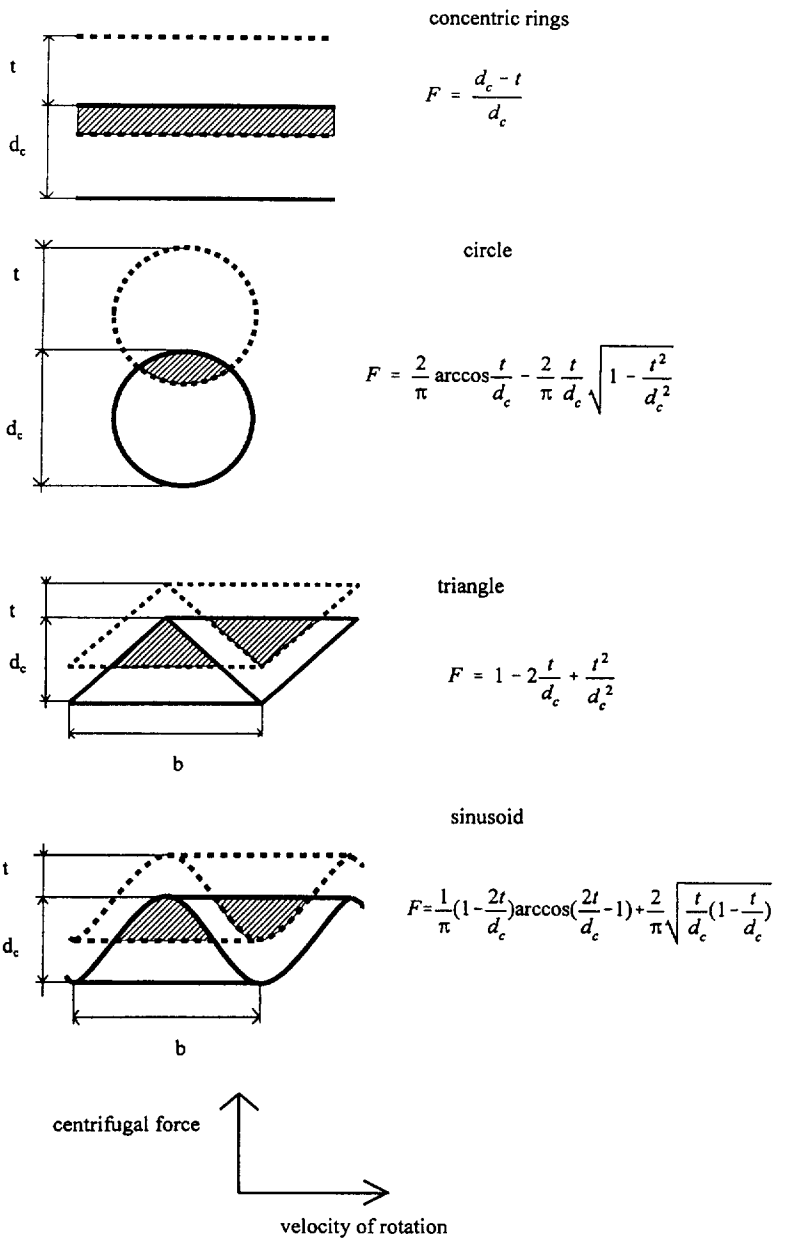

Fig. 3. Centrifugally induced particle displacement in channels of different shapes.

the channel entrance is now equal to the ratio of the shaded area formed by the overlap of the previously discussed two cross-sectional areas and the area of the channel itself. This ratio, denoted by F, depends on the ratio of the radial particle displacement t to the radial width of the separation channel d_c and has been determined for the four types of separation channels under consideration (Fig. 3).

Explicit expressions for the particle collection efficiency E can now be constructed, noting that

$$E = 1 - F \tag{6}$$

where F is a function of the ratio t/d_c as indicated in Fig. 3. For this ratio we can write

$$\frac{t}{d_c} = \frac{u_p}{u_{p100\%}} \tag{7}$$

where u_p is the radial velocity with which particles of diameter d_p move, specified by Eq. (2), while $u_{p100\%}$ is the radial migration velocity of the particles which are collected with 100% efficiency, specified by Eq. (3). Upon using Eq. (4) we have

$$\frac{t}{d_c} = \frac{d_p^2}{d_{p100\%}^2} \tag{8}$$

Using Eqs. (6) and (8) and the results given in Fig. 3, the following explicit descriptions for the particle collection efficiency as a function of the dimensionless particle diameter

$$x = d_p / d_{p100\%} \tag{9}$$

are obtained:

concentric rings

$$E = \begin{cases} 1 & x \geq 1 \\ x^2 & x \leq 1 \end{cases} \tag{10}$$

circles

$$E = \begin{cases} 1 & x \geq 1 \\ \frac{2}{\pi} x^2 (1 - x^4)^{1/2} + \frac{2}{\pi} \arcsin x^2 & x \leq 1 \end{cases} \tag{11}$$

triangles

$$E = \begin{cases} 1 & x \geq 1 \\ 2x^2 - x^4 & x \leq 1 \end{cases} \tag{12}$$

sinusoids

$$E = \begin{cases} 1 & x \geq 1 \\ 1 - \pi^{-1} \left[(1 - 2x^2) \arccos(2x^2 - 1) + 2x(1 - x^2)^{1/2} \right] & x \leq 1 \end{cases} \tag{13}$$

Plots are presented in Fig. 4 of the above specified particle collection efficiency distributions as a function of the dimensionless particle diameter x. It is seen that for $x < 1$ the collection efficiency of circular, triangular and sinusoidal channels is larger than that of concentric rings. The degree of improvement is directly related to the degree to which the radial height of a particular shaped channel is less than its maximum height. Triangular channels have on average the shortest radial distance over which particles must travel, hence their efficiency is largest for $x < 1$, bearing in mind that x is non-dimensionlized with $d_{p100\%}$ based on maximum height.

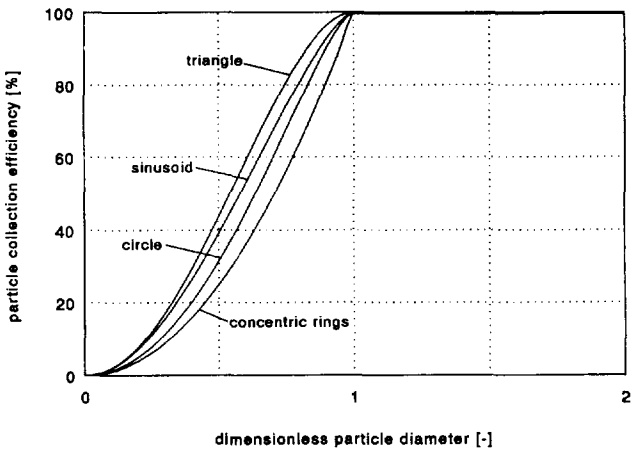

Fig. 4. Particle collection efficiency as a function of dimensionless particle diameter for a single separation channel with uniform axial velocity.

4. The effect of parabolic velocity profiles over the channel cross-section

In deriving the previous expressions for the particle collection efficiency as a function of particle diameter, it has been assumed that the axial velocity is constant in magnitude over the cross-section of the channel. Although such an assumption may be satisfied at the channel entrance, due to wall friction in combination with viscosity, with distance from the entrance the axial flow will evolve to a parabolic type of shape as a function of cross-sectional position. In the case of circular channels, this is known as Hagen–Poiseuille flow [5,6]. The effect of a parabolic shape on the particle collection efficiency distributions will be quantified below.

4.1. Concentric rings

A channel formed by two concentric rings is considered, where the gap between the rings, d_c, is small compared with their radii. Due to wall friction, the axial gas and particle velocity will depend on the radial distance μ from the inner ring at $\mu = 0$ to the outer ring at $\mu = d_c$:

$$w_{gas} = w(\mu) \qquad 0 \leq \mu \leq d_c \tag{14}$$

The trajectory of any particle which moves axially along the coordinate z with velocity w and radially, due to centrifugation, along the coordinate μ with velocity u_p can be described by the equation

$$\psi_p = \text{constant} \tag{15}$$

where ψ_p is the stream function defined as

$$\psi_p = \int_{d_c}^{\mu} w(\mu)\, d\mu + (L-z)u_p \qquad (16)$$

where z is the axial distance and L the length of the separation channel. The stream function is such that at the collecting wall of the separation channel, i.e. at $\mu = d_c$ and $z \le L$, the value of the stream function is positive. In other words, particles which reach the collecting wall follow streamlines which correspond to positive values of the stream function.

The collection efficiency of particles of specific diameter entering the separation channel is defined as the fraction of particles of such a diameter which reach the collecting wall. The geographic distribution of the flowing particles of a specific diameter as a function of μ at the channel entrance will be directly proportional to $w(\mu)$. The particle collection efficiency will then be equal to

$$E = \frac{\int_{\alpha}^{d_c} w\, d\mu}{\int_{0}^{d_c} w\, d\mu} \qquad \alpha \ge 0 \qquad (17)$$

where the integration range $\alpha \le \mu \le d_c$ corresponds to that area of the channel entrance where ψ_p is positive. Particles entering the channel in this area will be able to reach the collecting wall. The value of α thus follows from the condition that $\psi_p(z=0) = 0$. Using solution Eq. (16), this is equivalent to

$$\int_{\alpha}^{d_c} w\, d\mu = u_p L \qquad (18)$$

An expression for the particle collection efficiency is now obtained by substituting Eq. (18) into the right-hand side of Eq. (17). Thereby, it is noted that, if $\alpha \le 0$, all particles in the cross-sectional area of the channel entrance will reach the wall: $E = 1$ if $\alpha < 0$. Furthermore, it is noted that the average axial velocity in the channel is defined as

$$\bar{w} = \frac{1}{d_c}\int_{0}^{d_c} w\, d\mu \qquad (19)$$

As a result, the following expression for the particle collection efficiency is obtained:

$$E = \begin{cases} u_p L/\bar{w}d_c & \text{if } u_p \le \bar{w}d_c/L \\ 1 & \text{if } u_p \ge \bar{w}d_c/L \end{cases} \qquad (20)$$

Using the equation for the radial migration velocity of particles given by Eq. (2),

$$E = \begin{cases} d_p^2/d_{p100\%}^2 & d_p \le d_{p100\%} \\ 1 & d_p \ge d_{p100\%} \end{cases} \qquad (21)$$

where $d_{p100\%}$ is given by Eq. (4) with $w_{gas} = \bar{w}$.

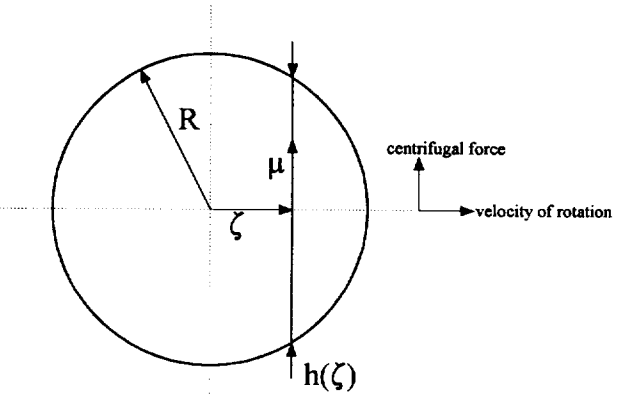

Fig. 5. Local coordinates in the circular channel.

The above result is identical to the previously given expression for the particle collection efficiency in the case of concentric rings (cf. Eqs. (9) and (10)) provided one takes $w_{gas} = \bar{w}$ in the expression for $d_{p100\%}$ (cf. Eq. (4)). It can thus be concluded that, for separation channels formed by concentric rings, the particle collection efficiency is independent of the shape of the axial flow in such channels, i.e. the previously given formulae for concentric rings still apply provided one takes a value for the axial velocity which corresponds to the average axial velocity through the channel.

4.2. Circles

To derive an expression for the particle collection efficiency in the case of a circular separation channel, it is convenient to distinguish the system of parallel planes in such a channel within which the movement of the particles takes place (Fig. 5). These planes are constituted by the longitudinal axis, along which the gas and particles move, and the transverse or radial axis with respect to the centre of rotation, along which particles move as a result of centrifugation. In such planes, which are perpendicular to the direction of the velocity of rotation, the results of the previous section for concentric rings apply provided that $d_{p100\%}$ is based on local conditions, i.e.

$$E_\zeta = \begin{cases} 1 & d_p \ge d_{p100\%}(\zeta) \\ d_p^2/d_{p100\%}^2(\zeta) & d_p \le d_{p100\%}(\zeta) \end{cases} \qquad (22)$$

where ζ is the coordinate perpendicular to the system of parallel planes defining the position of any such plane within the circular channel (Fig. 5). The value of $d_{p100\%}(\zeta)$ is given by Eq. (4) where w_{gas} is equal to $\bar{w}(\zeta)$, the average axial velocity in the plane located at position ζ, and d_c is equal to $h(\zeta)$, the distance between the walls of the circular channel at position ζ:

$$h(\zeta) = 2(R^2 - \zeta^2)^{1/2} \qquad (23)$$

The axial velocity distribution in a circular channel corresponds to Hagen–Poiseuille flow [5,6] which can be described in terms of the local Cartesian coordinates ζ and μ as

$$w(\mu, \zeta) = 2w_a\left(1 - \frac{\mu^2 + \zeta^2}{R^2}\right) \tag{24}$$

where w_a is the axial velocity averaged over the entire cross-section, μ is the coordinate perpendicular to ζ, i.e. in the direction of the centrifugal force, $-h/2 \le \mu \le h/2$, and R is the channel radius (Fig. 5). The average axial velocity in planes ζ = constant is given by

$$\bar{w}(\zeta) = h^{-1} \int_{-h/2}^{h/2} w(\mu, \zeta)\, \mathrm{d}\mu = \frac{4}{3} w_a\left(1 - \frac{\zeta^2}{R^2}\right) \tag{25}$$

The particle collection efficiency distribution for the circular channel can now be determined by weighting the contribution of all planes in such a channel as

$$E = \frac{\int_{-R}^{+R} E_\zeta h\bar{w}\, \mathrm{d}\zeta}{\int_{-R}^{+R} h\bar{w}\, \mathrm{d}\zeta} \tag{26}$$

Using the above results for E_ζ and $h\bar{w}$, one obtains, after some algebraic manipulation, the expression for the particle collection efficiency distribution in circular channels subject to Hagen–Poiseuille flow:

$$E = \begin{cases} 1 & x \ge (4/3)^{1/2} \\ \frac{4}{\pi}x^2 a - \frac{4}{3\pi}(1-a^2)^{1/2} a\left(\frac{5}{2} - a^2\right) - \frac{2}{\pi}\left(\arcsin a - \frac{\pi}{2}\right) & x \le (4/3)^{1/2} \end{cases} \tag{27}$$

where

$$a = [1 - (3x^2/4)^{2/3}]^{1/2} \tag{28}$$

The dimensionless particle diameter x is given by Eq. (9) wherein $d_{p100\%}$ is given by Eq. (4) with w_{gas} equal to the average axial channel velocity and d_c equal to the diameter of the circle forming the channel.

Plots are presented in Fig. 6 of the particle collection efficiency distribution appropriate for circular channels in the case of a uniform axial velocity profile and in the case of a parabolic (Hagen–Poiseuille type) velocity profile. Deviations are apparent in the area around $x = 1$ and $x < (4/3)^{1/2}$. For $x \to 0$, both efficiency distributions become identical.

4.3. Triangles

In the case of a channel with a triangular cross-section (or any other cross-section) the particle collection efficiency distribution for parabolic flow profiles can be assessed in a similar manner as for circular channels presented above. Again, planes can be distinguished within which particles move and for such planes the results obtained for concentric rings can be applied (cf. Eq. (22)). The overall efficiency can be

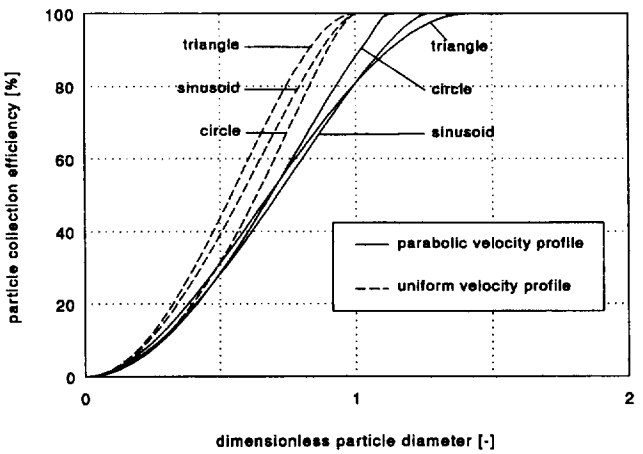

Fig. 6. Particle collection efficiency as a function of dimensionless particle diameter for a single separation channel considering uniform and parabolic axial velocity profiles inside the channel.

determined by weighting over all planes analogous to Eq. (26).

To execute the above procedure the velocity profile in the channel needs to be known. Explicit descriptions for such profiles are known in the case of equilateral and isosceles triangles with a top angle of 90° [7]. Furthermore, by making use of the results for the mathematically analogous problem of elastic torsion of equally shaped massive bars, asymptotic approximations are available for the case of isosceles triangles with a height d_c which is much smaller than the base width b. For such triangles the axial velocity profile can be described by

$$w = 12w_a(\mu h - \mu^2)/d_c^2 \qquad 0 \le \mu \le h \tag{29}$$

where w_a is the axial velocity averaged over the entire cross-section, μ is the coordinate perpendicular to the base, i.e. in the direction of the centrifugal force, and h is the local height of the triangle:

$$h = d_c - \frac{2|\zeta| d_c}{b} \qquad -\frac{b}{2} \le \zeta \le \frac{b}{2} \tag{30}$$

where ζ is the coordinate along the base and b is the base width (Fig. 3).

Upon using solution Eq. (29), valid for $d_c \ll b$, the particle collection efficiency distribution appropriate for viscous flow can be derived as

$$E = \begin{cases} 1 & x \ge \sqrt{2} \\ 2x^2\left[1 - \frac{3}{4}\left(\frac{x^2}{2}\right)^{1/3}\right] & x \le \sqrt{2} \end{cases} \tag{31}$$

The dimensionless particle diameter x is given by Eq. (9) wherein $d_{p100\%}$ is given by Eq. (4) with w_{gas} equal to the average axial channel velocity and d_c equal to the height of the triangle.

Plots are presented in Fig. 6 of the particle collection efficiency distribution appropriate for triangular channels in the case of a constant axial velocity profile (cf. Eq. (12)) and

in the case of a parabolic flow profile (cf. Eq. (31)). Some deviations are seen for values around $x=1$ and $x<\sqrt{2}$. For $x\to 0$, both efficiency distributions become identical.

4.4. *Sinusoids*

As for circular and triangular channels, for channels formed by sinusoidal waves of the type shown in Fig. 3 planes can also be distinguished within which the particles move. In each of such planes, the particle collection efficiency can be described by Eq. (22) wherein $d_{p100\%}$ is defined by Eq. (4) with w_{gas} equal to the average axial velocity at the location of the plane under consideration (analogous to Eq. (25) for the circular channel) and d_c equal to the local height of the channel at the location of the plane under consideration (analogous to Eq. (23) for the circular channel). The overall efficiency, taking account of all parallel planes, can be calculated analogous to Eq. (26). For the axial velocity profile we take a parabolic profile analogous to that for the triangular channel:

$$w=(48/5)w_a(\mu h-\mu^2)/{d_c}^2 \qquad 0\le\mu\le h \tag{32}$$

where w_a is the axial velocity averaged over the entire channel cross-section and h is the local height of the sinusoidal channel:

$$h=\frac{d_c}{2}+\frac{d_c}{2}\cos\frac{2\pi\zeta}{b} \qquad -\frac{b}{2}\le\zeta\le\frac{b}{2} \tag{33}$$

where b is the wavelength and d_c is the maximum channel height. Analogous to the triangle, it can be shown that the parabolic description of the velocity profile given by Eq. (32) is a good approximation for Hagen–Poiseuille type flow in sinusoidally shaped channels when the height d_c is much less than the width b.

Using the above results, the particle collection efficiency appropriate for sinusoidally shaped channels with a parabolic velocity profile is obtained as

$$E=\begin{cases}1 & x\ge\sqrt{8/5}\\ 1+\pi^{-1}(2x^2-1)\arccos[(5x^2)^{1/3}-1]-\dfrac{1}{15\pi}[5(5x^2)^{1/3}+15+2(5x^2)^{2/3}][2(5x^2)^{1/3}-(5x^2)^{2/3}]^{1/2} & x\le\sqrt{8/5}\end{cases} \tag{34}$$

Here, x is given by Eq. (9) wherein $d_{p100\%}$ is defined by Eq. (4) with w_{gas} equal to the average axial channel velocity and d_c equal to the maximum height of the channel.

Plots are presented in Fig. 6 of the particle collection efficiency appropriate for sinusoidally shaped channels in the case of constant and parabolic axial velocity profiles.

With regard to the results presented in this section the following general observations can be made. For concentric rings, the efficiency distribution is independent of the radial shape of the velocity profile. For circular, triangular and sinusoidal channels, however, the development of a parabolic velocity profile leads to some reduction of the efficiency in the area where x is about unity (see Fig. 6). The underlying reason is that, for channels of varying radial height, the average axial velocity in the radial plane where the radial height of the channel is largest, e.g. in Eq. (25) at $\zeta=0$, is greater than the average axial velocity for the channel as a whole, namely, by a factor 4/3, 2 and 8/5 for circular, triangular and sinusoidal channels, respectively. It is for this reason that the efficiency reaches its maximum of unity for values of x larger than unity, i.e. at $x=\sqrt{4/3}$, $\sqrt{2}$ and $\sqrt{8/5}$ for circular, triangular and sinusoidal channels, respectively.

5. The effect of different axial gas flow distributions over a multitude of separation channels

The descriptions for the particle collection efficiency given in the previous sections were derived considering a single channel. For a filter element consisting of a multitude of separation channels, as for example shown in Fig. 1, the separation process taking place in each channel will be equivalent for all channels if the axial gas velocity w_{gas} is proportional to the distance of the channel from the rotation axis r, i.e. $w_{gas}\propto r$. In this case $d_{p100\%}$ is equal for all channels and the previously given distributions can be applied to the filter element as a whole, taking for $d_{p100\%}$ the value calculated from Eq. (5).

If the gas flow distribution is different from the above indicated linear one, the degree of particle separation in each channel will be different. The particle collection efficiency of the assembly of channels will be a combination of the distributions appropriate for the individual channels. The form of the combined distribution is assessed as follows.

The total amount of particles entering each channel per unit time can be assumed to be proportional to the magnitude of the axial flow through that channel. Therefore, the overall efficiency of an assembly of separation channels can be assumed to be equal to the collection efficiency of the individual channels weighted according to the magnitude of the axial flow over these channels:

$$E_o=\phi^{-1}\int_{\theta=0}^{2\pi}\int_{r=R_i}^{R_o} Ewr\,dr\,d\theta \tag{35}$$

where ϕ is the gas flow through the filter element, r the radial distance ($R_i \le r \le R_o$), θ the azimuthal angle ($0 \le \theta \le 2\pi$), w the axial flow at position (r, θ) and E the collection efficiency of the separation channel at position (r, θ). Explicit descriptions for E as a function of $d_p/d_{p100\%}$ have been given in the previous sections, wherein the dependence of $d_{p100\%}$ from r and θ follows from Eq. (4).

To asses the effect of axial flow distributions which deviate from the previously discussed linear one, the following cases are considered: a flow which is constant with respect to r and θ, i.e. $w \propto 1$, and a flow which is linearly proportional to the product of r and θ, i.e. $w \propto r\theta$. Here, the case $w \propto 1$ is exemplary for the situation where the pressure drop over the channels is very large such that a constant distribution of the flow over the channels results. The case $w \propto r\theta$ may reflect a flow situation occurring in the case of impeller blades fitted upstream and/or downstream of the filter element. In the case of a limited number of impeller blades the axial gas flow can change in magnitude in the tangential direction, going from the pressure side to the suction side of the blades. This process repeats itself in each filter segment between two successive blades. As the particle collection efficiency appropriate for each segment is the same, its effect can be represented by a single dependence of w_{gas} on θ, i.e. $w_{gas} \propto r\theta$, $0 \le \theta \le 2\pi$.

For the cases $w \propto 1$ and $w \propto r\theta$, the right-hand side of Eq. (35) has been evaluated considering both concentric and triangular separation channels. In evaluating Eq. (35) in the case of concentric rings, use has been made of solution Eq. (10) which is valid irrespective of the shape of the velocity profile inside the channels. In the case of triangular channels, solution Eq. (31) has been used which is applicable for parabolic velocity profiles inside such channels.

Concentric rings

$w \propto 1$:

$$E_o = \begin{cases} 1 & x \ge \beta_i^{-1/2} \\ (\beta_o^2 - \beta_i^2)^{-1}\left(\beta_o^2 - \dfrac{1}{3x^4} - \dfrac{2}{3}\beta_i^3 x^2\right) & \beta_o^{-1/2} \le x \le \beta_i^{-1/2} \\ x^2 & x \le \beta_o^{-1/2} \end{cases} \tag{36}$$

$w \propto r\theta$:

$$E_o = \begin{cases} 1 & x \ge 2^{1/2} \\ x^2 - \dfrac{1}{4}x^4 & x \le 2^{1/2} \end{cases} \tag{37}$$

Triangles

$w \propto 1$:

$$E_o = \begin{cases} 1 & x \ge (2/\beta_i)^{1/2} \\ (\beta_o^2 - \beta_i^2)^{-1}\left[\beta_o^2 - \dfrac{8}{15x^4} - \dfrac{4}{3}x^2\beta_i^3 + \dfrac{9}{5}\beta_i^{10/3}\left(\dfrac{x^2}{2}\right)^{4/3}\right] & (2/\beta_o)^{1/2} \le x \le (2/\beta_i)^{1/2} \\ 2x^2\left[1 - \dfrac{9}{20}(\beta_o^2 - \beta_i^2)^{-1}(\beta_o^{10/3} - \beta_i^{10/3})\left(\dfrac{x^2}{2}\right)^{1/3}\right] & x \le (2/\beta_o)^{1/2} \end{cases} \tag{38}$$

$w \propto r\theta$:

$$E_o = \begin{cases} 1 & x \ge 2 \\ 2x^2 + \dfrac{1}{8}x^4 - 9\left(\dfrac{x^2}{4}\right)^{4/3} & x \le 2 \end{cases} \tag{39}$$

where

$$\beta_i = \frac{3R_i(R_o + R_i)}{2(R_o^2 + R_oR_i + R_i^2)}, \quad \beta_o = \frac{3R_o(R_o + R_i)}{2(R_o^2 + R_oR_i + R_i^2)} \tag{40}$$

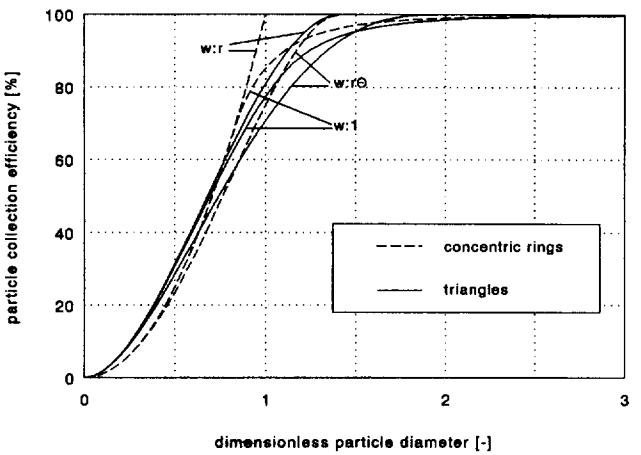

Fig. 7. Particle collection efficiency as a function of dimensionless particle diameter for an assembly of channels considering various flow distributions over the assembly.

while x is the particle diameter non-dimensionalized by $d_{p100\%}$ (cf. Eq. (9)), with $d_{p100\%}$ defined by Eq. (5).

Plots are presented in Fig. 7 of the above particle collection efficiency as a function of the dimensionless particle diameter x. For the case of a constant axial flow distribution over the filter element, $w \propto 1$, the channels are taken to extend up to the rotation axis, i.e. $R_i = 0$, so that $\beta_i = 0$ and $\beta_o = 3/2$. From the curves it is seen that the lower tails, $x \to 0$, of the distributions are hardly affected by deviations from the optimum axial flow distribution over the filter element ($w \propto r$). The effect of deviations from the optimum flow distribution is mainly apparent in the value of the collection efficiency for particles with diameters of around $d_{p100\%}$. Furthermore, it is noted that the distributions appropriate for the case of a constant axial flow distribution approach a value of 100% only asymptotically as $x \to \infty$. This is a reflection of the leakage of particles through channels located near and at the rotation axis where separation is small or absent altogether. If the separation channels do not extend up to the rotation axis, $R_i > 0$, the efficiency is equal to unity for $x \geq \beta_i^{1/2}$ and $x \geq (2/\beta_i)^{1/2}$ for concentric rings and triangular channels, respectively (cf. Eqs. (36) and (38)).

6. Corrections for molecular flow effects

In deriving an expression for the radial migration velocity of particles in a centrifugal field (see Eq. (1)), use was made of Stokes' law to describe the resistance force acting on the particle in the case of relative movement. Stokes' law, however, does not take into account the effects of molecular flow apparent when the particle diameter becomes of the same order of magnitude or smaller than the mean free path of the gas. In that case, Stokes' law can be corrected using the Cunningham correction factor [8]. The expression for the radial migration velocity given by Eq. (2) becomes, in corrected form,

$$u_p = \rho_p \frac{d_p^2 \Omega^2 r}{18\eta}\left(1 + \frac{2.52\lambda}{d_p}\right) \tag{41}$$

where λ is the mean free path. For air at standard (room) temperature and pressure, $\lambda = 0.066$ μm.

Using Eqs. (3) and (41), one can derive an improved expression for the diameter of the smallest particle which is collected with 100% efficiency in a channel with uniform axial velocity:

$$d^*_{p100\%} = d_{p100\%}[(1 + c^2)^{1/2} - c] \tag{42}$$

where $d_{p100\%}$ is given by Eq. (4) and c represents the correction for molecular flow effects, defined as

$$c = 1.26\lambda / d_{p100\%} \tag{43}$$

Solution Eqs. (9)–(13) are descriptions of the particle collection efficiency as a function of the dimensionless particle diameter x valid for a single channel with uniform axial velocity. As follows from the derivation of these solutions (cf. Eqs. (7), (8) and (9)), they are valid irrespective of the form of the resistance force acting on a particle in the case of relative movement, provided x is defined as

$$x = \left(\frac{u_p}{u_{p100\%}}\right)^{1/2} \tag{44}$$

where u_p is the radial migration velocity of the particle and $u_{p100\%}$ is defined by Eq. (3). Using Eqs. (41)–(43), Eq. (44) becomes

$$x = \left[\left(\frac{d_p}{d_{p100\%}}\right)^2 + 2c\frac{d_p}{d_{p100\%}}\right]^{1/2} \tag{45}$$

while the inverse of this relation is

$$d_p = [(x^2 + c^2)^{1/2} - c]\, d_{p100\%} \tag{46}$$

The above equations provide relations between the particle diameter d_p and the variable x within which the effect of molecular flow is properly taken into account. They can be applied unrestrictedly to the expressions for particle collection efficiency distributions as a function of x for single channels with uniform axial velocity. Moreover, it can be shown that Eqs. (45) and (46) can equally well be applied to the solutions for particle collection efficiency valid for a single channel with parabolic axial velocity profile (cf. Eqs. (21), (27), (31) and (34)), and for a multitude of channels (cf. Eqs. (36)–(40)). Consistent with previous definitions, for the solutions valid for parabolic axial velocity profiles in a single channel, $d_{p100\%}$ is defined by Eq. (4) with w_{gas} equal to the average axial velocity inside the channel; for the solutions valid for a multitude of channels, $d_{p100\%}$ is defined by Eq. (5). The results thus obtained properly take account of molecular flow effects as described by Eq. (41).

It is noted that for $c \ll x$, Eq. (46) can be approximated as

$$d_p \sim x d_{p100\%} - 1.26\lambda \tag{47}$$

In other words, if $c \ll x$, the effect of molecular flow can be represented by a shift in particle diameter of 1.26λ. For air at

standard temperature and pressure, $1.26\lambda = 0.083$ μm. Eq. (47) then implies that, due to molecular flow effects, particles collected with a specific efficiency become 0.083 μm smaller. In general, it can be stated that the effects of molecular flow lead to improved separation. The improvement becomes noticeable for particles in the submicrometre range.

7. Experimental evidence

The separation performance of the rotational particle separator has been tested under various circumstances. Concentrations at the inlet and outlet as a function of particle diameter were measured using cascade impactors and laser particle counter techniques. In this way, collection efficiencies for particles with diameters of 0.1 μm and larger could be assessed.

Two types of design of the rotational particle separator were employed, namely, a rotational particle separator with tangential inlet (Fig. 8) and a rotational particle separator with axial inlet (Fig. 9). The version with the tangential inlet is suited to gases with high dust concentrations. The cyclone type tangential inlet serves as a preseparation device within which course particle material is separated from the gas

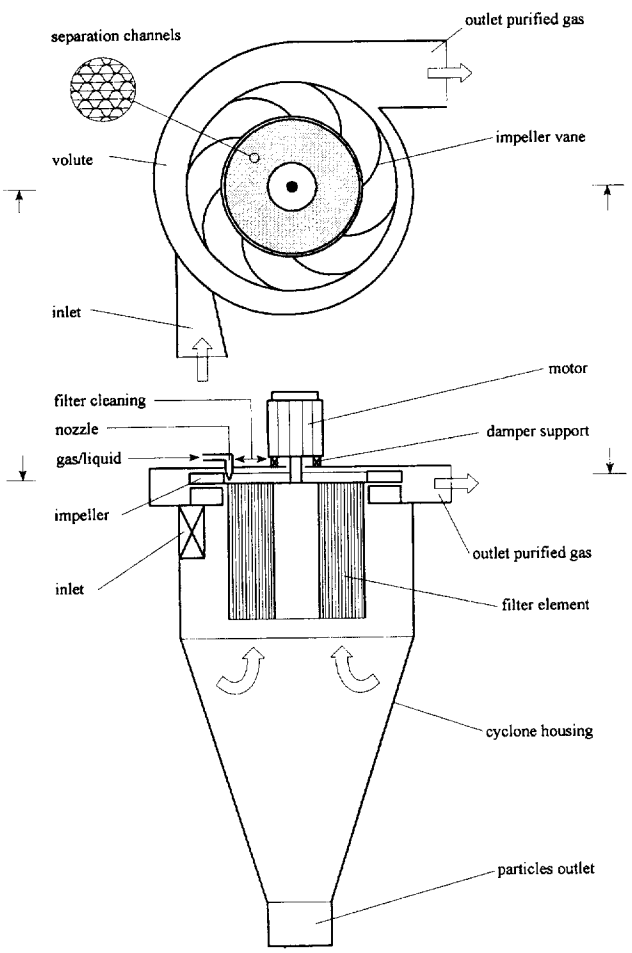

Fig. 8. Tangential version of the rotational particle separator.

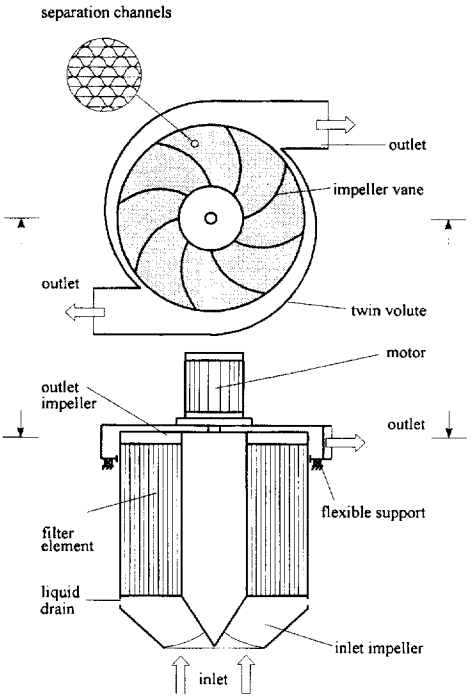

Fig. 9. Axial version of the rotational particle separator.

before entry into the separation channels where fine particles are centrifuged. In the version with the axial inlet a preseparation device is absent. This version is more compact and suited to gases with low concentrations of fine dust particles.

In total, six rotational particle separators were tested, three of the axial type and three of the tangential type. Measurements were executed at various laboratories. Data on test conditions and rotational particle separators used are presented in Table 1.

Results obtained for the particle collection efficiency are presented in Fig. 10. Here, the experimentally assessed particle collection efficiency has been plotted against the corrected dimensionless particle diameter defined by Eqs. (45) and (46) with $d_{p100\%}$ defined by Eq. (5). The value of $d_{p100\%}$ calculated for each rotational particle separator tested is given in Table 1.

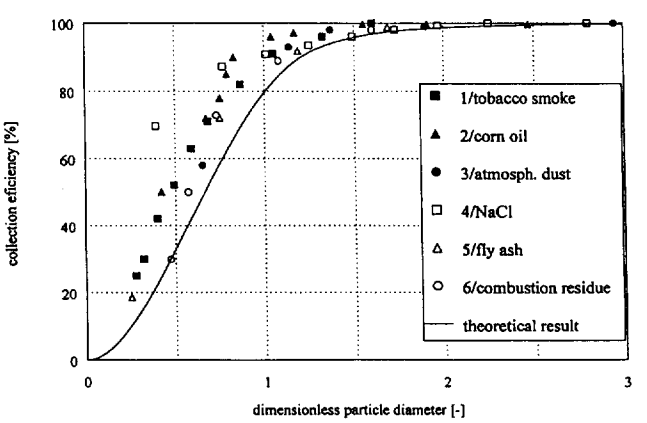

Fig. 10. Experimentally and theoretically assessed particle collection efficiency as a function of dimensionless particle diameter.

Table 1
Data of tests with six rotational particle separators

Case	1	2	3	4	5	6
Particle material	tobacco smoke	corn oil	atmospheric dust	sodium chloride	fly ash	combustion residue
Carrier gas	air	air	open air	air	flue gas	air
Temperature	20°C	20°C	−20 to +30°C	20°C	200°C	20°C
Particle density	900 kg/m^3	900 kg/m^3	2000 kg/m^3	2165 kg/m^3	2500 kg/m^3	1000 kg/m^3
Mean particle diameter	0.25 μm	0.1–0.2 μm		3.3 μm	10 μm	3.5 μm
Inlet concentration	±0.5 mg/m^3	1.6×10^6 particles	±50 μg/m^3	3.8 g/m^3	5 g/m^3	1.6 g/m^3
Measurement technique	laser spectrometer PMS ASAS-300A	laser spectrometer PMS 101	laser spectrometer Met One 237B	cascade impactor Andersen 1ACFM	cascade impactor Andersen Mark-3	cascade impactor Andersen 1ACFM
Rotational particle separator data						
Version	axial	axial	axial	tangential	tangential	tangential
Filter length	0.22 m	0.66 m	1.0 m	0.31 m	0.3 m	0.18 m
Filter diameter	0.26 m	0.55 m	1.36 m	0.25 m	0.60 m	0.31 m
Channel height	0.73 mm	1.4 mm	2.3 mm	2.2 mm	2.2 mm	1.5 mm
Area reduction	0.27	0.15	0.11	0.11	0.11	0.10
Angular velocity	250 rad/s	300 rad/s	75 rad/s	300 rad/s	150 rad/s	300 rad/s
Actual air flow	0.056 m^3/s	0.328 m^3/s	2.78 m^3/s	0.042 m^3/s	0.45 m^3/s	0.194 m^3/s
$d_{p100\%}$ (Eq. (5))	0.55 μm	0.27 μm	0.57 μm	0.42 μm	0.76 μm	0.98 μm

In addition to the experimental results, the theoretical distribution given by Eq. (38) with $\beta_i = 0$ is shown in Fig. 10. This distribution applies to triangularly shaped channels with a parabolic velocity profile inside the channels, the flow being constant in magnitude over all channels. The underlying reasons for choosing this distribution as reference for the experimental results are as follows.

(i) For the rotational particle separators tested, the distribution of the flow over the channels was not the optimum one corresponding to $w \propto r$. As a conservative and reasonable approximation, $w \propto 1$ has been chosen. Furthermore, the inner radius R_i of the filter element was in most cases small compared with the outer radius, hence $R_i = \beta_i = 0$ was conservatively taken.

(ii) For all the rotational particle separators considered, the entry length at which the velocity profile evolves to a parabolic profile [5] is a fraction of the total channel length. A parabolic profile is representative of the velocity field over the largest part of the channels.

(iii) In all cases the shape of the channels was sinusoidal or almost sinusoidal with a height to wavelength ratio of approximately 0.3. It has been found impossible to develop expressions in closed form from Eq. (35) in the case of sinusoidally shaped channels and $w \propto 1$. However, as can be verified from Figs. 4 and 6, results for triangularly shaped channels are a good approximation to those for sinusoidally shaped channels.

From the results presented in Fig. 10 it is seen that theoretically and experimentally established efficiency values are quite close. The theoretical curve tends to be on the conservative side of the experimental results. This can in most of the cases considered be attributed to the built-in conservatism in the theoretical curve including the assumed distribution for the flow over the filter element (Re(i)). For a number of rotational particle separators tested it was possible to define a more appropriate distribution for the flow over the filter element, the incorporation of which resulted in yet better correspondence between experiment and theory.

8. Conclusions

In general, it can be concluded that the separation of particles in the rotational particle separator is a well-defined and quantifiable physical process. The degree of separation of specific designs can be assessed in advance.

Acknowledgements

The author wishes to thank the Management of Romico Hold for permission to publish the information contained in this article.

References

[1] J.J.H. Brouwers, *Chem. Eng. Technol., 19* (1996) 1–10.
[2] R.G. Dorman, *Dust Control and Engineering*, Pergamon, New York, 1974.
[3] A.G. Stern, *Air Pollution, Vol. IV: Engineering Control of Air Pollution*, Academic Press, New York, 1977.
[4] F. Löffler, *Chem.-Ing.-Tech., 60* (1988) 443–452.
[5] R.B. Bird, W.E. Stewart and E.N. Lightfoot, *Transport Phenomena*, Wiley, New York, 1960.
[6] H. Schlichting, *Boundary-Layer Theory*, McGraw-Hill, New York, 1979.
[7] R. Berker, Integration des equations du mouvement d'un fluide visqueux incompressible, *Encyclopedia of Physics*, Vol. VIII/2, Springer, Berlin, 1963.
[8] W.C. Hinds, *Aerosol Technology*, Wiley, New York, 1982.